Chemistry
A European
Journal

Chemistry Europe
European Chemical Societies Publishing

Accepted Article

Title: The synthesis and mechanistic considerations of a series of ammonium monosubstituted H-phosphonate salts

Authors: Erin Leitao, Keng Lung Lee, Joey Feld, Paul Hume, and Tilo Söhnel

To be cited as: *Chem. Eur. J.* 10.1002/chem.202003090

Link to VoR: https://doi.org/10.1002/chem.202003090

WILEY-VCH

10.1002/chem.202003090

WILEY-VCH

FULL PAPER

The synthesis and mechanistic considerations of a series of ammonium monosubstituted *H*-phosphonate salts

Keng Lung Lee,[a],[c] Joey Feld,[a] Paul Hume,[b],[c] Tilo Söhnel[a],[c] and Erin Leitao *[a],[c]

[a] Mr KL Lee, Mr J Feld, A/Prof T Söhnel, Dr EM Leitao
School of Chemical Sciences
University of Auckland
Private Bag, 92019, Auckland, 1142, New Zealand
E-mail: erin.leitao@auckland.ac.nz
[b] Dr P Hume
School of Chemical and Physical Sciences
Victoria University of Wellington
Wellington, New Zealand
[c] The MacDiarmid Institute for Advanced Materials and Nanotechnology
New Zealand

Supporting information for this article is given via a link at the end of the document.

Abstract: A series of ammonium monosubstituted *H*-phosphonate salts were synthesized by combining *H*-phosphonate diesters with amines in the absence of solvent at 80°C. Variation of the ester substituent and amine produced a range of ionic liquids with low melting points. The products and by-products were analyzed by spectroscopic and spectrometric techniques in order to get a better mechanistic picture of the dealkylation and *formal* dearylation observed. For dialkyl *H*-phosphonate diesters, $(RO)_2P(O)H$ (R = alkyl), the reaction proceeds via direct dealkylation with the reactivity increasing in the order R = *i*-Pr < Et < Me corresponding to DFT calculated activation enthalpies of 22.6, 20.8, and 17.9 kcal/mol. For the diphenyl *H*-phosphonate diesters, $(PhO)_2P(O)H$, the dearylation was found to proceed via phenol-assisted formation of a 5-coordinate intermediate, $(PhO)_3PH(OH)$, from which $P(OPh)_3$ and water were eliminated. The presence of an equivalent of water then facilitated the formation of $P(OH)_2OPh$ and the amine, $R'NH_2$, subsequently abstracted a proton from it to yield $[(PhO)PH(O)O]^-[R'NH_3]^+$.

Introduction

H-phosphonate diesters are phosphorus compounds that are characterised by the presence of multiple functional groups: P-OR, P-H and P=O.[1] These molecules have attracted a lot of attention in both organic and inorganic chemistry for the creation of new phosphorus element bonds, such as P-N,[2], P-O-P and P-P,[3], P-F,[4], P-S, P-Se and P-Te,[5] and P-C bonds[6] due to their interesting reactivity as both the phosphorus centre and α-carbon can be subject to nucleophilic attack. More recently, *H*-phosphonate diesters have been used in the formation of molecules[7] and macromolecules[8] with interesting architectures and useful potential applications.

One of the most beneficial features of *H*-phosphonate diesters is their ability to undergo tautomerization similar to keto-enol tautomerization. The tautomeric equilibrium exists between a five-coordinated phosphonate, P(V) ($\lambda^5\sigma^4$), and three-coordinated phosphite, P(III) ($\lambda^3\sigma^3$), favouring the P(V) tautomer over the P(III) tautomer (**Figure 1**).[9] The equilibrium position is influenced by the substituents on the *H*-phosphonate diesters. For instance, substituents with strong electron-withdrawing effects (e.g. R = Ph) help to stabilise the lone pair in the P(III) tautomer, making the *H*-phosphonates more reactive. By contrast, electron-donating substituents (e.g R = Me, Et and *i*-Pr) destabilise the lone pair, and the equilibrium lies heavily towards the P(V) tautomer, making the *H*-phosphonate diesters less reactive.[10] Tautomerization is the first step when *H*-phosphonates are attacked by a nucleophile such as an alcohol,[11] water,[12] or an amine[13] and lead to the formal exchange of the OR substituent with the nucleophile (e.g. OR', OH, or NHR', respectively).[14]

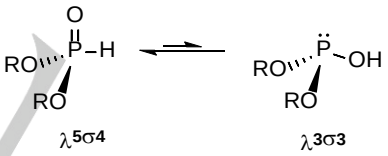

Figure 1. Tautomerization of *H*-phosphonate diesters P(V), to disubstituted phosphite, P(III).

The vast majority of the reported reaction chemistry of *H*-phosphonate diesters is *via* nucleophilic attack at the phosphorus center, however, the α-carbon atom on the OR substituent, is also susceptible to nucleophilic attack. For example, this reaction can lead to abstraction of an alkyl group on *H*-phosphonates to form an anion when reacted with an amine (e.g. $[(RO)PH(O)O]^-$ **Scheme 1**). Initially, these anions were postulated to be too reactive to exist under standard conditions but were theoretically predicted to be stabilized by hydrogen bonding with the alkylated amine cation, forming an ionic salt.[1a] Subsequently, these salts have been postulated as intermediates in the Atherton-Todd reaction,[15] can be synthesized through direct dealkylation reactions of *H*-phosphonate diesters and amines,[16] and have been observed as by-products when *H*-phosphonates are used as precursors in the synthesis of phosphoramidates *via* copper-catalysed dehydrogenative coupling.[2d] In the latter, as the reaction involves the use of an amine as a substrate, the reaction efficiency suffers as the formation of the ionic salt is competitive with the dehydrogenative coupling reaction.

10.1002/chem.202003090

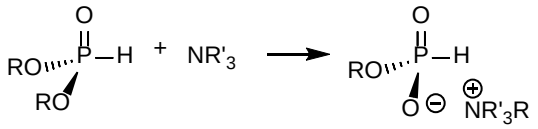

Scheme 1. Alkylation of an amine by dialkyl *H*-phosphonate.

Formation of ionic liquids, ionic materials with melting points lower than 100°C, such as alkylphosphonate imidazolium salts, are also possible through direct dealkylation of *H*-phosphonate diesters. Ionic liquids with a phosphonate anion exhibit high conductivities (ca. 10^{-3} S cm^{-1} at 25°C) which is correlated with low glass-transition temperatures.[17] Due to the nature of the anion, it is possible to form multiple complexes with the imidazolium cation. These solvents have excellent reactivity towards copper, exhibit substantial corrosion protection of magnesium alloys,[18] are potential CO_2 absorbents[19], can extract polysaccharides from Japanese cedar[20] and are used as synthons in making new *H*-phosphonates.[21]

Unlike monodealkylation with dialkyl *H*-phosphonates, monodearylation from diphenyl *H*-phosphonate is not possible due the absence of an electrophilic α-carbon available for nucleophilic attack. Instead, diphenyl *H*-phosphonate has been postulated to undergo a disproportionation reaction to form a monophenyl *H*-phosphonate anion and triphenylphosphite in the presence of base (**Scheme 2**).[22]

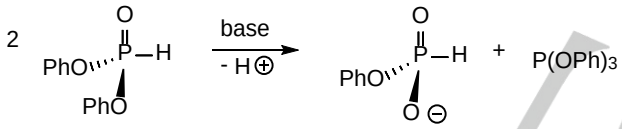

Scheme 2. Base catalysed disproportionation of diphenyl *H*-phosphonate.

To improve the selectivity and efficiency during the synthesis of ammonium monosubstituted *H*-phosphonate salts as well as in oxidative dehydrogenative coupling reactions between *H*-phosphonates and amines, it is crucial to understand the formation of these ionic salts. In this work, a series of monosubstituted *H*-phosphonate ammonium salts were synthesized and characterized, including by thermogravimetric analysis and mass spectrometry. To gain insight into the mechanisms, kinetic studies were performed by monitoring the phosphorus-containing compounds using ^{31}P NMR spectroscopy. Spectroscopic and spectrometric techniques were combined in order to observe the presence of any intermediates during the formation of the ion-pair and the experimental results were supported by DFT calculations.

Results and Discussion

Synthesis and characterization of ammonium monosubstituted *H*-phosphonate salts

A series of ammonium monosubstituted *H*-phosphonate salts were synthesized by combining the two components, *H*-phosphonate diester (**1**) and amine, in the absence of solvent at 80°C for 20 h (**2-4**, **Scheme 3**, **Figures S1-S22**). By ^{31}P NMR spectroscopy, a distinctive doublet can be observed due to the P-H bond in the anion, $[(RO)PH(O)O]^-$ (δ_P = 1.3-11.5 ppm, $^1J_{PH}$ = 611-664 Hz), with further splitting observed depending on the R group (**Table 1**). For example, the characteristic doublet of pentets of $(EtO)_2P(O)H$, **1b**, at 7.3 ppm ($^1J_{HP}$ = 680 Hz; $^3J_{PH}$ = 7.9 Hz, coupling to four CH_2 protons) was replaced with a doublet of triplets at 3.9 ppm, corresponding to the anion, $[(EtO)PH(O)O]^-$, in **2b** ($^1J_{PH}$ = 616 Hz; $^3J_{PH}$ = 8.0 Hz, coupling to two CH_2 protons) over time, as evidenced by ^{31}P NMR spectroscopy (**Figure S2**). The ^{31}P NMR peak assignment for **2b** is corroborated by a doublet signal (δ_H = 6.63 ppm, $^1J_{HP}$ = 616 Hz) observed in the ^{1}H NMR spectrum (**Figure S1**). Across the series, the observed coupling constants and chemical shifts for the various derivatives differ, thus are influenced by the interaction of the different cations as well as the attached R groups (e.g. Me, Et, *i*-Pr, Ph). Despite compounds **2b** and **3b** having the same anion, $[(EtO)PH(O)O]^-$, and the compounds in the series **2d**, **3d** and **4d**, $[(PhO)PH(O)O]^-$, there are notable differences in the ^{31}P NMR chemical shifts, at 3.9 and 3.6 ppm (**2b**, **3b** respectively) and 1.3, 1.4, 2.1 ppm (**2d**, **3d**, **4d** respectively). H-bonding in the form of N-H----O-P between the cation and anion is prevalent (see **Figures 2-3**) and inevitability contributes to the observed changes.

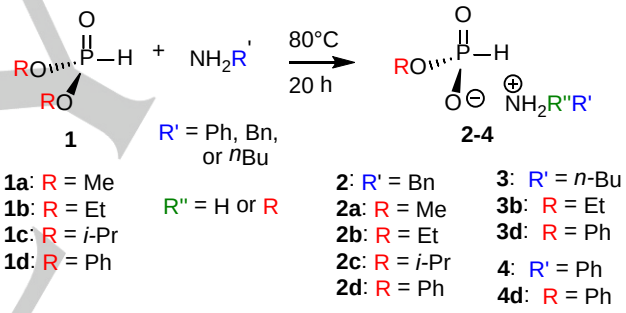

Scheme 3. Formation of a series of monosubsituted phosphonate salts (**2-4**) from the corresponding *H*-phosphonate diesters (**1**) and amines.

Table 1. Selected data for compounds **2-4**.

Compound	R/R'/R''	δ_P P-H /ppm ($^1J_{PH}$ /Hz)	Conversion[a] or Yield[b] /%
2a	Me/Bn/mix	11.5 (617)	80[a]
2b	Et/Bn/mix	3.9 (616)	83[a]
2c	*i*-Pr/Bn/mix	6.4 (614)	16[a]
2d	Ph/Bn/H	1.3 (645)	45[b],[c]
3b	Et/Bu/mix	3.6 (611)	78[a]
3d	Ph/Bu/H	1.4 (644)	48[a],[c]
4d	Ph/Ph/H	2.1 (664)	40[b],[c]

[a] conversion as determined by ^{31}P NMR spectroscopy after 20 hours of reaction time at 80°C (**2a** was at 20°C). [b] isolated yield after recrystallization. [c] maximum yield/conversion = 50% due to the formation of $P(OPh)_3$ during the synthesis.

10.1002/chem.202003090

The ammonium cations, $[R'R''NH_2]^+$, in the monosubstituted *H*-phosphonate salts can be characterized by using a mixture of ^{1}H NMR spectroscopy and ESI mass spectrometry. The ammonium cation of compound **2b** was observed as a mixture of $[BnNH_3]^+$ and $[BnEtNH_2]^+$. Two quartets (δ_H = 2.7-3.8 ppm, $^3J_{HH}$ = 7.1 Hz) and two triplets (δ_H = 1.1-1.4 ppm, $^3J_{HH}$ = 7.1 Hz), one corresponding to the Et group on the cation, $[BnEtNH_2]^+$, and the other corresponding to the Et group on the anion, $[(EtO)PH(O)O]^-$ were observed by ^{1}H NMR spectroscopy (**Figure S1**). This assignment was also supported by ESI mass spectrometry ($[C_9H_{16}NO_3P + H]^+$ 218.0946 *m/z* (cal'd 218.0946 *m/z*), $[C_{11}H_{20}NO_3P + H]^+$ 246.1254 *m/z* (cal'd 246.1254 *m/z*), **Figure S3**). However, the presence of a mixture of cations precludes purification for compounds **2a**, **2b**, **3b**. To account for the observation that *either* a proton or an ethyl group was *formally* transferred to the amine, either a one-step or a two-step route to the cations is possible (**Scheme 4**).

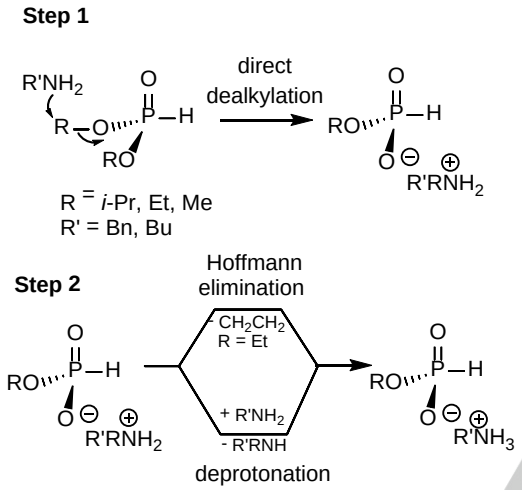

Scheme 4. One-step and two-step routes to forming ammonium cations.

The one-step route involves the direct transfer of the alkyl group, R, from $(RO)_2P(O)H$ via nucleophilic attack from the amine (Step 1, **Scheme 4** producing $[R'RNH_2]^+$). There are two options for the second step to produce the protonated ammonium cation, $[R'NH_3]^+$ i) Hoffmann elimination of the alkene directly from $[R'RNH_2]^+$ (e.g. for R = Et, loss of CH_2=CH_2)[23] or ii) deprotonation of the ammonium salt (e.g. $[R'RNH_2]^+$) via a second equivalent of base ($R'NH_2$) to yield R'RNH and $[R'NH_3]^+$ (Step 2, **Scheme 4**).[16a] The presence of mixed cations due to alkyl transfer in the series was limited to starting with either **1a** ($(MeO)_2P(O)H$), **1b** ($(EtO)_2P(O)H$) or **1c** ($(i\text{-}PrO)_2P(O)H$) and the Ph groups from **1d**, was not observed to be transferred to the ammonium cation (see **Figures S10** and **S18**). This suggests that a different mechanism is in operation for the diphenyl *H*-phosphonate, **1d**, resulting in exclusively the ammonium cation, $[R'NH_3]^+$, in compound **2d**. Unlike the dialkyl *H*-phosphonates, the α-carbon atom of diphenyl *H*-phosphonate is not vulnerable to nucleophilic attack so direct dearylation of the amine is not possible. Instead, during the synthesis of the series **2d**, **3d**, **4d**, another significant resonance was observed by ^{31}P NMR spectroscopy at 128.0 ppm, corresponding to $P(OPh)_3$ agreeing with the previously reported studies on the base catalyzed disproportionation of **1d** (**Scheme 2**, and Mechanistic considerations).[22] Due to the generation of $P(OPh)_3$ and PhOH during the synthesis (which is also present in trace amounts in the starting material, **1d**, observed by ^{1}H NMR spectroscopy), the maximum conversion (or yield) possible when starting with compound **1d** is 50% (**Table 1**).

Single crystals were grown for the ammonium phenyl *H*-phosphonate salts, **2d** and **4d**, by slow diffusion of hexanes into a saturated dichloromethane solution; the crystal structures were solved by single crystal X-ray diffraction (**Figures 2-3**, **S23-S24 Tables S1-S3**). From the molecular structures, both the P and N centres exhibit slightly distorted tetrahedral geometry as the smallest bond angle is 102.48(8)° and the largest is 120.21(9)° (**Figures 2a** and **3a**).

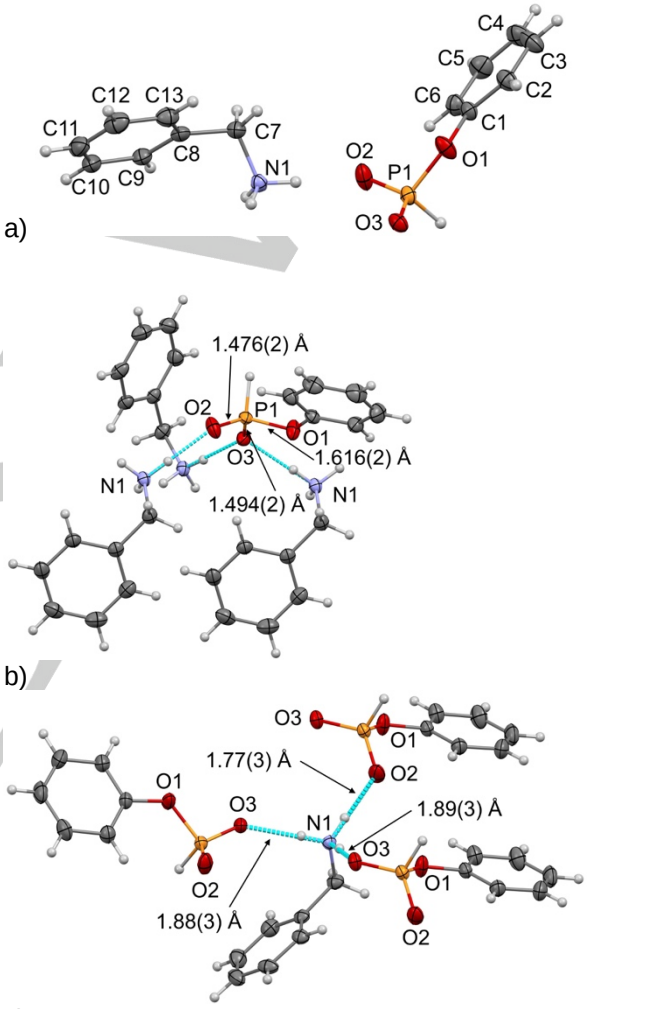

Figure 2. Molecular structure of **2d** showing a) the separated ion pair b) hydrogen bonding from the perspective of the ammonium cation c) hydrogen bonding from the prospective of the phosphate anion, with thermal ellipsoids shown at the 50% probability level.

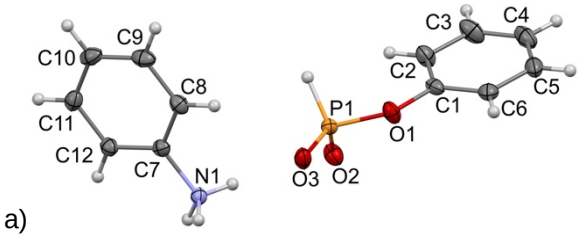

10.1002/chem.202003090

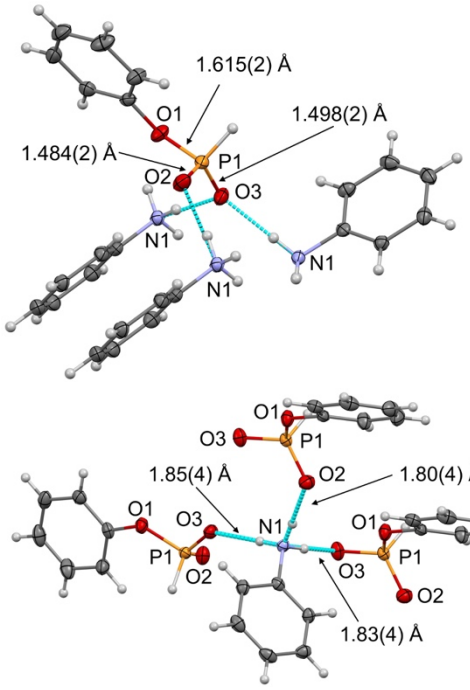

Figure 3. Molecular structure of **4d** showing a) the separated ion pair b) hydrogen bonding from the perspective of the ammonium cation c) hydrogen bonding from the prospective of the phosphate anion, with thermal ellipsoids shown at the 50% probability level.

The three P-O bonds in the anions have bond lengths of 1.616(2) Å and 1.615(2) Å (P1-O1(Ph), single bond), 1.476(2) Å and 1.484(2) Å (P1-O2 with more double bond character), and 1.494(2) Å and 1.498(2) Å (P1-O3 with more single bond character) for compounds **2d** and **4d**, respectively. Kee *et al.* reported similar ionic compounds with comparable P-O distances.[16a] For example, the anion $[(BnO)PH(O)H]^-$ has a P-O(Bn) distance of 1.590(1) Å and the other P-O bond lengths are 1.479(1) Å and 1.504(1) Å. However, when the anion is protonated, as in (ArO)PH(O)OH (Ar = 2,6-dimethylphenyl) synthesized by Murugavel *et al.*, the three bond lengths are 1.579(2) Å (P-O(Ar)), 1.527(2) Å (P-O(H)) and 1.469(2) Å (P=O), suggesting that both of the P-O bonds without substituents in **2d** and **4d** fall somewhere between double bonds and single bonds.[24] The ion pairs are held together with a substantial amount of H-bonding. From the perspective of the anion, $[PhOPH(O)O]^-$, the oxygens, O2, with more double bond character are bonded to one cation and the anionic oxygens, O3, are H-bonded to two cations (**Figures 2b** and **3b**). The cation, $[R'NH_3]^+$ (R' = Bn, Ph), containing three hydrogens is H-bonded to three anions with O-H distances of 1.77(3) Å, 1.88(3) Å and 1.89(3) Å for **2d** (**Figure 2c**) and distances of 1.80(4) Å, 1.83(4) Å and 1.84(4) Å for **4d** (**Figure 3c**).

Compounds **2a-c** and **3b** are viscous liquids and therefore could have utility as protic ionic liquids.[18-19, 25] To compare with similar *H*-phosphonate ionic liquids, thermogravimetric analysis (TGA) was performed on the products (**Figures S4, S11, S15, S19, S22**). However, the ionic salts suffered some weight loss at relatively low temperatures (38-100°C) which is not commonly observed for these types of ionic salts. It is postulated, in this case, that the trace amounts of amines and impurities present in the compounds (see **Figures S1-S22**) resulted in evaporation at a lower temperature. Moreover, all the TGA spectra showed a steep increase in mass loss at 100°C which is characteristic for water loss. Considering the reactions were performed without using any solvents, this suggests that the ionic liquids are quite hygroscopic, capturing moisture from the atmosphere. As an alternative explanation, protic ionic liquids sometimes exist in equilibrium with their respective neutral compounds (**Figure 4**) and this equilibrium causes the loss of electrostatic forces of attraction making the liquid more volatile. Lastly, full decomposition of all of the compounds was not observed even at 600°C, which is unusual compared to other protic ionic liquids reported on literature.[25]

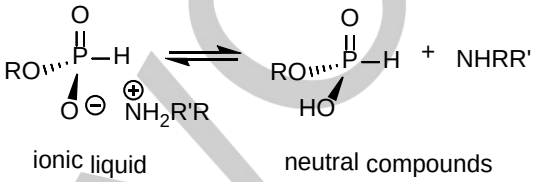

Figure 4. Protic ionic liquids, such as ammonium monoalkyl *H*-phosphonate, in equilibrium with the starting acid and base.

Prior to running TGA, the melting points of **2d** and **4d** were determined to be 112.3°C and 116.4°C, respectively (**Table 2**). For the viscous liquids **2b**, **3b**, and **3d** it was crudely determined that melting points are below 0°C. Compound **2d** had the highest T_{peak} which was 222°C. The TGA curve for **2d** also showed consistent loss of mass starting from 50°C and the compound started to decompose at T_{onset}= 131°C. By contrast, **4d** experienced mass loss starting from 56°C, which is in agreement with the instability observed both in solution and in the solid state (**Figure S22**). In addition, compound **4d** had the lowest T_{peak} at 161°C and the lowest T_{onset} at 113°C. For compound **3d**, the TGA curve depicted multistage decomposition, with T_{onset} at 125°C and the maximum rate of weight loss at T_{peak} = 181°C (**Figure S19**). Compounds **2b** and **3b** showed similar decomposition curves with identical T_{onset} at 162°C and T_{peak} at 181°C (**Figures S4 and S15**).

Table 2. Decomposition temperatures for selected ionic salts

Compound	T_{onset} /°C	T_{peak} /°C	Melting point /°C
2b	162	181	< 0
2d	131	222	11.3
3b	162	181	< 0
3d	125	181	< 0
4d	113	161	116.4

According to a review paper published by Cao and Mu,[26] five levels of thermal stability can be categorized based on the value of T_{onset}. When T_{onset} is lower than 250°C, the thermal stability of ionic liquids is classified as *least stable* while the *most stable* ionic liquids are those that possessed T_{onset} greater than 400°C. This suggests that the ionic liquids formed from *H*-phosphonate and amines are among the least thermally stable and this will limit their applications. Furthermore, the authors compared the relationship between thermal stability and chain length. Although the effect of

chain length was not significant, it was clear that the shorter chain length tends to have higher thermal stability. The was rationalized as, even though a longer chain length can increase Van der Waals forces, the bulky structure minimizes the electrostatic interaction between the cation and anion.[26]

Mechanistic considerations

For the series of compounds produced by monodealkylation of **1a-c** using benzylamine, **2a-c**, the reactions were monitored over time by ^{31}P NMR spectroscopy. Dimethyl *H*-phosphonate, **1a**, reacted with benzylamine within minutes at 80°C, so for this derivative, the temperature was reduced to 20°C. Consistent with what was reported by Troev *et al.*[23a] a doublet of quartets for **2a** (δ_P = 11.5 ppm, $^1J_{PH}$ = 619 Hz, $^3J_{PH}$ = 12 Hz) was observed by ^{31}P NMR spectroscopy (**Table 2**, **Figure S25**). An intermediate aminolysis product,[14] **5a** ((MeO)(BnNH)P(O)H, δ_P = 14.2 ppm, $^1J_{PH}$ = 696 Hz, $^3J_{PH}$ = 12 Hz **Scheme 5**) was also observed at early reaction times as a doublet of sextets in the ^{31}P NMR spectra (**Table 3**) and then disappeared after 7 hours. ESI-MS analysis and ^{1}H NMR spectroscopy were performed on the sample after the timed experiment, revealing that the cation in **1a** was a mixture of $[BnMeNH_2]^+$, $[BnMe_3N]^+$ and $[BnNH_3]^+$(**Figures S26-S27**) with the $[(MeO)PH(O)O]^-$ anion visible in the negative infusion spectrum (**Figure S28**). Presence of $[BnMe_3N]^+$ is presumably possible by first demethylating **1a** to form $[BnMeNH_2]^+$ which can be deprotonated by $BnNH_2$ to form $[BnNH_3]^+$ along with the stronger nucleophile, BnMeNH. Then the 2° amine can demethylate another molecule of **1a** to generate $[BnMe_2NH]^+$ and the deprotonation/demethylation steps can occur once more to yield the quaternary ammonium cation, $[BnMe_3N]^+$. After integrating the ^{31}P{^{1}H} NMR spectra over time and plotting the relative integrations, the initial rate of formation of **2a** was found to be 0.006 min^{-1} at 20°C (**Figure S29**).

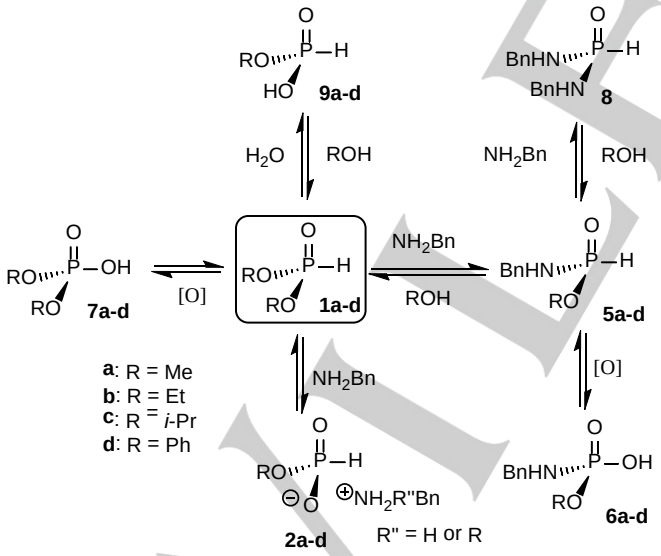

a: R = Me
b: R = Et
c: R = *i*-Pr
d: R = Ph

Scheme 5. Aminoloysis, hydrolysis, alcoholysis, and oxidation of **1** as postulated routes to the intermediates observed during the synthesis ionic salts **2**.

The reaction of diethyl *H*-phosphonate, **1b**, with benzylamine took 4 days to reach completion at 80°C. Similar to **2a**, **2b** was observed as a doublet of triplets (δ_P = 9.0 ppm, $^1J_{PH}$ = 615 Hz, $^3J_{PH}$ = 8.2 Hz) by ^{31}P NMR spectroscopy (**Table 3**, **Figure S30**). The intermediate aminolysis product, **5b** ((EtO)(BnNH)P(O)H, δ_P = 17.7 ppm, $^1J_{PH}$ = 637 Hz, $^3J_{PH}$ = 9.4 Hz **Scheme 5**) was detected as a doublet of pentets in the ^{31}P NMR spectrum, reached its highest concentration at 60 minutes when it could be detected by ESI-MS ($[C_9H_{14}NO_3P + Na]^+$ 222.0662 *m/z* (cal'd 222.0660 *m/z*), **Figure S31**) and then slowly disappeared over 7 hours. The presence of a persistent by-product, **6b**, ((EtO)(BnNH)P(O)OH, δ_P = 28.6 ppm) was also observed during the reaction of **1b** with benzylamine. The initial rate for formation of **2b** was determined to be 0.131 min^{-1} at 80°C (**Figure S32**).

Table 3. Intermediates and products formed during the kinetic monitoring of the conversion of **1** to **2**

Starting Material	Intermediate or Product	δ_P P-H /ppm, splitting, $^1J_{HP}$ /Hz, $^3J_{HP}$ /Hz,
1a	**2a**	11.5, dq, 619, 12
1a	**5a**	14.2, ds, 696, 12
1b	**2b**	9.0, dt, 615, 8.2
1b	**5b**	17.7, dp, 637, 9.4
1b	**6b**	28.6, tt
1c	**2c**	7.0, dd, 613, 9.5
1c	**5c**	15.5, br d, 635
1c	**6c**	26.9. dt
1c	**7c**	3.7, br s
1d	**2d**	6.6, d, 645
1d	**5d**	9.2, dt, 716, 9.3
1d	**8**	17.7, ds, 647, 10.5
1d	**9d**	15.7, d, 667
1d	$P(OPh)_3$	128, s

[a] conversion as determined by ^{31}P NMR spectroscopy after 20 hours of reaction time at 80°C. [b] maximum conversion = 50% due to the formation of $P(OPh)_3$ during the synthesis.

Moving from diethyl to diisopropyl *H*-phosphonate resulted to an increase in the number of side reactions possible (**Table 3**, **Figures S33-S36**). As with the synthesis of **2a** and **2b**, an aminolysis intermediate, **5c** ((*i*-PrO)(BnNH)P(O)H, δ_P = 15.5 ppm, $^1J_{PH}$ = 635 Hz **Scheme 5**) was observed as a broad doublet by ^{31}P NMR spectroscopy at early reaction times reaching its maximum concentration in solution at 180 minutes before disappearing. The aminolysis reaction was more competitive in the reaction with **1c** relative to **1a** and **1b**, due to the presence of the bulky isopropyl groups that inhibits nucleophilic attack at the *α*-carbon. However, based on the observations of previous reactions, the aminolysed products are unstable and exist in equilibrium with the reactants, eventually favouring the formation of more thermodynamic product, **2**. By-products **6c** ((*i*-PrO)(BnNH)P(O)OH, δ_P = 26.9 ppm) and a minor amount of **7c** ((*i*-PrO)$_2$P(O)OH, δ_P = 3.7 ppm) were also spectroscopically observed (**Figure S36**). After the course of the reaction, the main species present was **2d** (**Figure S37**) containing both the protonated and alkylated ammonium cations ($[BnNH_3]^+$ and [Bn(*i*-

Pr)NH_2]$^+$) as observed by ESI mass spectrometry (**Figures S38**). The reaction between diisopropyl *H*-phosphonate, **1c**, with benzylamine to form **2c** was more than two orders of magnitude slower than the formation of **2b** at 80°C with an initial rate of 0.001 min^{-1} (**Figure S39**). Furthermore, unlike with **2a** and **2b**, the reaction between **1c** and benzylamine did not reach completion after 7 days at 80°C and approximately 22% of **1c** remained unreacted with only 51% of **2c** formed along with 16% of **6c**.

Diphenyl *H*-phosphonate, **1d**, reacted with benzylamine instantly when the two reactants were mixed together at 20°C. After 30 s of stirring, about 94% of **1d** was consumed to produce various phosphorus compounds according to numerous peaks in the ^{31}P NMR spectra (**Table 3**, **Scheme 5**, **Figure S40-S42**), including $P(OPh)_3$ (δ_P =128.0 ppm) as a major product. Among all of these phosphorus species, **2d** (δ_P = 6.6 ppm, $^1J_{PH}$ = 645 Hz) comprised 37% of the total mixture. Interestingly, three signals corresponding to **5d** ((PhO)(BnNH)P(O)H, δ_P = 9.2 ppm, $^1J_{PH}$ = 716 Hz, $^3J_{PH}$ = 9.3 Hz), **9d** ((HO)(BnNH)P(O)H δ_P =15.8 ppm, $^1J_{PH}$ = 667 Hz,) and **8** ($(BnNH)_2P(O)H$, δ_P = 17.7 ppm, $^1J_{PH}$ = 647 Hz, $^3J_{PH}$ = 10.5 Hz) were observed by ^{31}P NMR spectroscopy during the initial stages of the reaction, but slowly diminished over time (**Scheme 5**). To assist with the aforementioned assignments, the ESI mass spectrum at 30 min revealed two major phosphorus species [$(BnNH_2)$(PhO)P(O)H + Na]$^+$ (**5d**) and [$(BnNH_2)_2$P(O)H + H]$^+$ (**8**) (**Figure S42**) which were not observed in the end of the reaction. Both of these intermediates were the result of aminolysis substitution reactions. As the PhO substituent has a stronger electron withdrawing effect on the *H*-phosphonate when compared with alkyoxy substituent, tautomerization, and hence aminolysis, is favoured.

Overall, the order of reactivity for the various *H*-phosphonate diesters with benzylamine follows the trend: **1d** > **1a** > **1b** > **1c**. In addition to comparing the difference in the reactivity by modifying the R group, it is also possible to modify the nucleophilicity of the amine (**Scheme 6**). Reacting diethyl *H*-phosphonate, **1b**, with amines $BnNH_2$, *n*-$BuNH_2$ and Et_3N produced the corresponding ammonium ethyl *H*-phosphonate salts in 78% (**2b**), 83% (**3b**), and 19% conversion (**10b**) after 20 h at 80°C, respectively (**Table 4**, **Figures S43-S44**). These results indicate that the Et_3N is too sterically bulky to effectively monodealkylate **1b** and the two primary amines have similar nucleophilicity in this reaction. By ^{1}H NMR spectroscopy it was clear that **10b** contained a mixture of both [Et_4N]$^+$ and [Et_3NH]$^+$ cations. Reacting diphenyl *H*-phosphonate, **1d**, with the same three amines, $BnNH_2$, *n*-$BuNH_2$ and Et_3N, produced the corresponding ammonium phenyl *H*-phosphonate salts in 48% (**2d**), 45% (**3d**), and 14% conversion (**10d**) after 20 h at 80°C, respectively (**Table 4**, **Figures S44-S45**). In addition, starting from **1d**, $P(OPh)_3$ was produced, along with PhOH indicating that both of these species are involved in the mechanism. Additionally, all of the cations formed from **1d** are protonated amines (e.g. [$BnNH_3$]$^+$, [*n*-$BuNH_2$]$^+$, or [Et_3NH]$^+$).

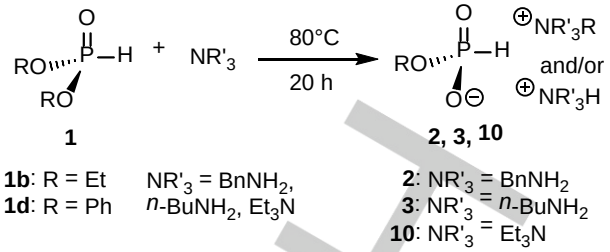

Scheme 6. Reaction comparison of **1b** and **1d** with different amines.

Table 4. The effect of the amine on the formation of the ammonium monosubstituted *H*-phosphonate salts

Starting Material	Amine	δ_P P-H /ppm ($^1J_{HP}$ /Hz)	Conversion[a] /%
1b	none	7.3 (680)	n/a
1b	*n*-$BuNH_2$	3.6 (611)	78
1b	$BnNH_2$	3.9 (616)	83
1b	Et_3N	4.4 (616)	19
1d	none	4.5 (669)	n/a
1d	*n*-$BuNH_2$	1.4 (644)	48[b]
1d	$BnNH_2$	1.3 (645)	45[b]
1d	Et_3N	1.9 (663)	14[b]

[a] conversion as determined by ^{31}P NMR spectroscopy after 20 hours of reaction time at 80°C. [b] maximum conversion = 50% due to the formation of $P(OPh)_3$ during the synthesis.

DFT Calculations

DFT calculations were performed in order to gain a deeper understanding of the underlying mechanism of salt formation. Calculations employed the B3LYP exchange-correlation functional,[27] with the 6-311+(d,p) basis set and Grimme's empirical dispersion correction (D3).[28] Solvent effects were included by the use of a polarizable continuum model (PCM). Dibutylamine was selected for the PCM because of its chemical similarity to benzylamine, and comparable dielectric constant.

For the alkyl (R = Me, Et, *i*-Pr) series **1a-c**, it was possible to locate transition states for direct nucleophilic dealkylation by benzylamine (**Scheme 7**). The activation enthalpies for these processes follow the trend expected from steric considerations (17.9, 20.8, and 22.6 kcal/mol for Me, Et, and *i*-Pr, respectively).

The possibility that compounds **5a-c** were intermediates in the formation of **2a-c** was considered. However, this interpretation is inconsistent with the observed reaction kinetics (see previous Section, and Supporting Information). The transient accumulation of **5a-c**, together with the fact that no other phosphorus-containing species were observed in significant quantities, means that consumption of **5a-c** would need to be rate-limiting under this hypothesis. This would imply that the rate of formation of **2a-2c** would increase with concentration of **5a-5c**, however this is not

10.1002/chem.202003090

the case. Therefore, the interpretation given in **Scheme 4**, is favored wherein reversible formation of **5a-5c** leads to an initial accumulation of these species, which are subsequently consumed as the irreversible formation of **2a-2c** proceeds. The observation of analogous species **5d** in the reaction of **2d** with $BnNH_2$, which follows a different mechanism, further supports this conclusion.

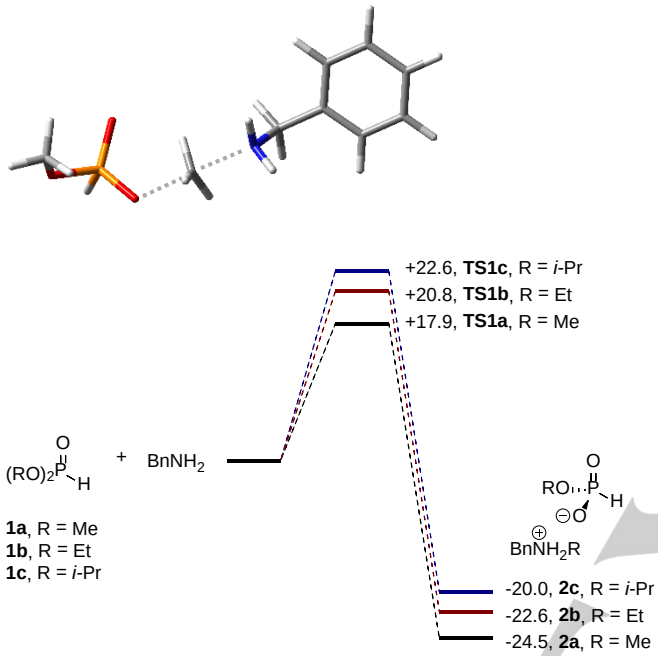

Scheme 7. Direct nucleophilic dealkylation of dialkyl *H*-phosphonates by $BnNH_2$ and calculated activation/reaction enthalphies. All values given in kcal/mol. Transition state diagram shown for **1a**, R = Me.

For compound **1d** (R = Ph) nucleophilic displacement is precluded by the nature of the substituent. In attempting to develop a mechanistic hypothesis for this reaction it was important to account for the formation of $P(OPh)_3$, which is rapidly generated. A proposal involving phosphonate disproportionation has previously been reported[22] (**Scheme 8**). However, this mechanism posits nucleophilic attack on a phosphite centre bonded to a more electrophilic phosphonate. All attempts to locate transition states corresponding to this step were unsuccessful.

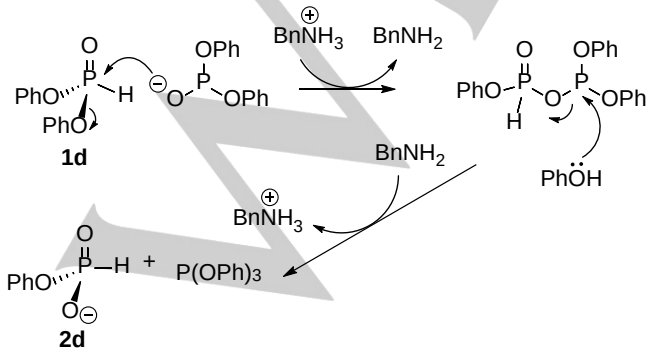

Scheme 8. Previously proposed mechanism for the formation of **2d** and $P(OPh)_3$.[22]

Instead, on the basis of previous work,[14] we propose that diphenyl *H*-phosphonate, **1d**, reacts with trace phenol (present in **2d**), which results in the formation of 5-membered intermediate, **Int-1**. Following pseudorotation, **Int-1** undergoes phenol-assisted dehydration to form $P(OPh)_3$ and water (**Scheme 9**). The water produced in this way can then react with a second equivalent of **1d** to form the corresponding five-membered intermediate **Int-2** and hydrolyse **1d** to **9d** (see also **Scheme 5**). DFT calculations indicate that the formation of five-membered intermediates **Int-1** and **Int-2** are associated with activation barriers of +15.8 and +27.4 kcal/mol respectively. Phenol-assisted loss of the apical substituent of five-membered intermediates **Int-1** and **Int-2** is associated with activation barriers of +10.7 and +7.6 kcal/mol, respectively. The high activation barrier associated with the formation of **Int-2** can be explained by activation of H_2O through H-bonding or protonation from the primary ammonium salt present in the mixture.

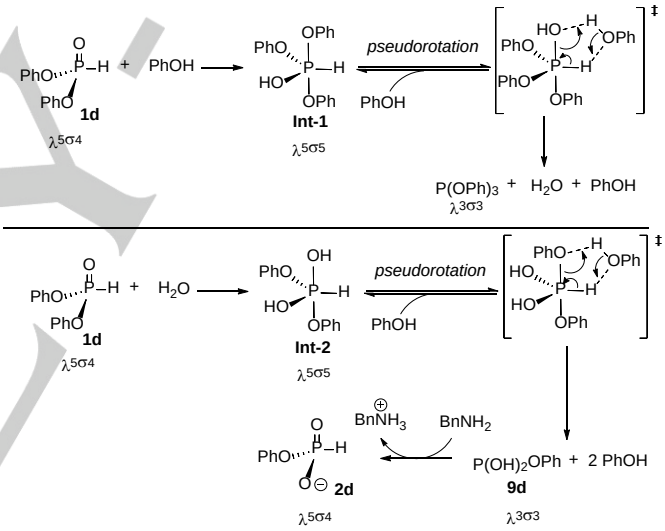

Scheme 9. Proposed mechanism for the formation of **2d** and $P(OPh)_3$ from **1d** in the presence of trace PhOH.

Conclusion

In summary, a series of ammonium monosubstituted *H*-phosphonate salts were prepared and thoroughly investigated by ESI-MS, multi-nuclear NMR spectroscopy, TGA and single crystal XRD, where appropriate. Evidence for the direct monodealkylation of $(RO)_2P(O)H$ (**1**) using both primary and tertiary amines, with the generation of a low concentration of the monoaminoloysis species, (RO)(NHR')P(O)H was observed for the series R = Me, Et, *i*-Pr. The rate of dealkylation experimentally followed the order Me > Et > *i*-Pr, corroborated by DFT calculations. A mixture of the protonated $[R'NH_3]^+$, and alkylated 2°, 3° and even 4° ammonium cations (e.g. $[R'RNH_2]^+$, $[R'R_2NH]^+$, $[R'R_3N]^+$, respectively) were observed for the dialkyl *H*-phosphonates.

Addition of amine to diphenyl H-phosphonate (**1d**), resulted to a relatively more complicated mixture on route to producing the ionic salt $[(PhO)PH(O)O]^-[BnNH_3]^+$ (**2d**). DFT calculations suggested that the presence of trace amounts of PhOH acts as an autocatalyst for the reaction eliminating H_2O from a 5-coordinate intermediate (**Int-1**). Hydrolysis of **1d** (via **Int-2**) then generated compound **9d** (observed experimentally) along with PhOH, followed by proton abstraction from the amine to afford product **2d**.

Understanding the ease of synthesis, the mechanistic details and selectivity in making ammonium monosubstituted *H*-phosphonate salts is key to using them as synthetic precursors for the creation of new *H*-phosphonates, such as heterodialkyl *H*-phosphonates,[21] or as other synthons, such as in the phosphorylation of chitosan.[29]

Experimental Section

General considerations and instrumentation.

All reagents and solvents were used as received from either Sigma-Aldrich or pH Scientific, unless otherwise stated. AR grade solvents were used. ^{1}H, ^{13}C, ^{31}P/^{31}P{^{1}H} NMR experiments were recorded using a Bruker Avance 400 MHz spectrometer. ^{1}H chemical shifts are recorded in parts per million (ppm) downfield tetramethylsilane and are referenced to residual protium in the NMR solvent (e.g. $CHCl_3$ δ = 7.26 ppm). Chemical shifts for carbon are reported in ppm relative to $CDCl_3$ (δ = 77.3 ppm). ^{31}P chemical shifts are reported in ppm relative to an external standard of 85% phosphoric acid (δ = 0 ppm). Data are represented as follows: chemical shift, multiplicity (app = apparent, br = broad, s = singlet, d = doublet, t = triplet, q = quartet, p = quintet, m = multiplet), coupling constants in Hertz (Hz), and integration. High resolution mass spectrometry measurements were made on a Bruker microTOF-QII mass spectrometer, equipped with a KD Scientific syringe pump, in positive ion ESI mode. Thermogravimetric analysis measurements were run with TA Instrument's thermogravimetric analyzer Model Q600 IR. The data was processed using TRIOS computer software connecting to the analyzer. TGA experiments were performed with the ramp rate of 10˚C/min up to 600˚C. 50 µL platinum pans (for liquid samples) and 100 µL ceramic pans (for solid samples) were used to contain the samples. X-ray diffraction measurements of single crystals (**2d** and **4d**) were performed on a Rigaku Oxford Diffraction XtaLAB-Synergy-S single-crystal diffractometer with a PILATUS 200K hybrid pixel array detector using Cu Kα radiation (λ = 1.54184 Å; Table S1). The data was processed with the SHELX2018/3[30] and Olex2 1.3[31] software packages. All non-hydrogen atoms were refined anisotropically. Mercury 2020.1[32] was used to visualize the molecular structure. All DFT calculations were done using Gaussian 09.[33] Note: due to the presence of by-products and multiple ammonium salts, compounds **2a** and **2c** were not isolated cleanly, however, were generated under the same conditions as **2b** and **2d** below.

Synthesis of ethyl *H*-phosphonate benzylammonium salt, 2b.
1b (5.0 mmol, 0.67 mL) and benzylamine (5.0 mmol, 0.55 mL) were added to a round bottom flask equipped with a stir bar. The mixture was stirred at 80°C for 20 hours. After the reaction, a DCM and hexane mixture was added to the mixture. The mixture was shaken and sonicated. The mixture was allowed to stand so the hexane and DCM mixture formed two layers. The product dissolved in the DCM layer. The hexane was decanted and the extraction process was repeated three times. The DCM and hexane residue was remove under vacuum overnight. A pale-yellow ionic liquid was formed. Conversion = 95% (some mixed ammonium salt remained preventing isolation and purification; see **Figures S1-S4**). ^{1}H NMR (400 MHz, $CDCl_3$): δ 7.28 – 7.50 (m, 5H), 6.63 (d, $^1J_{HP}$ = 616 Hz, 1H), 3.99 (s, 2H), 3.75 (m, 2 x 2H), 1.32 (t, $^3J_{HH}$ = 7.1 Hz, 3H) 1.20 (t, $^3J_{HH}$ = 7.1 Hz, 3H). ^{31}P NMR (162 MHz, $CDCl_3$): δ 3.9 (dt, $^1J_{PH}$ = 616 Hz, $^3J_{PH}$ = 8.0 Hz). ESI-MS: $[C_9H_{16}NO_3P + H]^+$ 218.0946 *m/z* (cal'd 218.0946 *m/z*), $[C_{11}H_{20}NO_3P + H]^+$ 246.1254 *m/z* (cal'd 246.1254 *m/z*), $[C_{11}H_{20}NO_3P + BnNH_2(Et)]^+$ 381.2297 *m/z* (cal'd 381.2297 *m/z*). T_{onset} = 162°C; T_{peak} = 188°C.

Synthesis of phenyl *H*-phosphonate benzylammonium salt, 2d.
1d (3.0 mmol, 0.57 mL) and benzylamine (3.0 mmol, 0.33 mL) were added to a round bottom flask equipped with a stir bar. The mixture was stirred at 80°C for 20 hours. After the reaction, solids precipitated and dichloromethane (DCM) was added to redissolve the solid. Hexane was added dropwise to form a layer on DCM. The mixture was allowed to recrystallize and the contents were filtered using a sintered filter funnel. The white crystalline solids were collected and dried under vacuum. Yield = 0.36 g (45%), mp = 112.3°C (see **Figures S5-S11, S23**). ^{1}H NMR (400 MHz, $CDCl_3$): δ 7.12-7.28 (m, 10H), 6.70 (d, $^1J_{HP}$ = 644 Hz, 1H), 3.70 (s, 2H). ^{1}H NMR (400 MHz, d_6-DMSO): δ 8.24 (s, 3H), 7.36-7.47 (m, 5H), 7.23 (t, $^3J_{HH}$ = 7.9 Hz, 2H), 7.05 (d, $^3J_{HH}$ = 8.3 Hz, 2H), 6.97 (t, $^3J_{HH}$ = 7.4 Hz, 1H), 6.83 (d, $^1J_{HP}$ = 593 Hz, 1H), 3.98 (s, 2H). ^{31}P NMR (162 MHz, $CDCl_3$): δ 1.3 (d, $^1J_{PH}$ = 645 Hz). ^{31}P NMR (162 MHz, d_6-DMSO): δ -2.5 (d, $^1J_{PH}$ = 593 Hz). ^{13}C{^{1}H} NMR (100.6 MHz, d_6-DMSO): δ 42.35, 120.36, 121.88, 128.30, 128.55, 128.75, 128.99, 134.5. ESI-MS: $[C_{13}H_{16}NO_3P + H]^+$ obs'd 266.0944 *m/z* (cal'd 266.0942 *m/z*), $[C_{13}H_{16}NO_3P + BnNH_3]^+$ 373.1668 *m/z* (cal'd 373.1676 *m/z*), $[2(C_{13}H_{16}NO_3P) + H]^+$ 531.1808 *m/z* (cal'd 531.1808 *m/z*), $[3(C_{13}H_{16}NO_3P) + H]^+$ 796.2649 *m/z* (cal'd 796.2676 *m/z*). T_{onset} = 131°C; T_{peak} = 222°C.

Synthesis of ethyl *H*-phosphonate *n*-butylammonium salt, 3b.
1b (5.0 mmol, 0.67 mL) and *n*-butylamine (5.0 mmol, 0.50 mL) were added to a round bottom flask equipped with a stir bar. The mixture was stirred at 80˚C for 20 hours. After the reaction, a DCM and hexane mixture was added to the mixture. The mixture was shaken and sonicated and the mixture was allowed to stand so the hexane and DCM mixture formed two layers. The product was dissolved in the DCM layer. The hexane layer was decanted and the extraction process was repeated three times. The DCM and hexane residue was remove under vacuum overnight. A colourless, viscous ionic liquid was formed. Conversion = 78% (some mixed ammonium salt remained preventing isolation and purification; see **Figures S12-S15**). ^{1}H NMR (400 MHz, $CDCl_3$): δ 8.61 (s, 3H), 6.78 (d, $^1J_{HP}$ = 611 Hz, 1H), 3.88 (p, $^3J_{HH}$ = 6.9 Hz, 2H), 2.90 (q, $^3J_{HH}$ = 7.0 Hz, 2H), 2.81 (m, 2H), 1.67 (m. 2H), 1.41 (m, 4H), 1.27 (t, $^3J_{HH}$ = 7.0 Hz, 3H), 0.94 (t, $^3J_{HH}$ = 7.5 Hz, 3H). ^{31}P NMR (162 MHz, $CDCl_3$): δ 3.6 (dt, $^1J_{PH}$ = 611 Hz, $^3J_{PH}$ = 8.1 Hz). ESI-MS: $[C_6H_{18}NO_3P + H]^+$ 184.1098 *m/z* (cal'd *m/z* 184.1097), $[C_6H_{18}NO_3P + H]^+$ 212.1414 *m/z* (cal'd *m/z* 212.1410), $[C_6H_{18}NO_3P + n\text{-}BuEtNH_2]^+$ 313.2614 *m/z* (cal'd 313.2615 *m/z*), $[2(C_6H_{18}NO_3P) + H]^+$ 423.2735 *m/z* (cal'd 423.2747 *m/z*). T_{onset} = 162°C; T_{peak} = 181°C.

Synthesis of phenyl *H*-phosphonate *n*-butylammonium salt, 3d.
1d (5.0 mmol, 0.95 mL) and *n*-butylamine (5.0 mmol, 0.50 mL) were added to a round bottom flask equipped with a stir bar. The mixture was stirred at 80°C for 20 hours. After the reaction, a DCM and hexane mixture was added. The mixture was shaken and sonicated. The mixture was allowed to stand so that hexane and DCM mixture formed two layers. The product was dissolved in the DCM layer. The hexane layer was decanted and the extraction process was repeated three times. The DCM and hexane residue was remove under vacuum overnight. The peach coloured ionic liquid was formed. Conversion = 48% (presence of phenol and $P(OPh)_3$ remained preventing isolation and purification; see **Figures S16-S19**). ^{1}H NMR (400 MHz, $CDCl_3$): δ 7.40 (s, 3H), 7.00-7.30 (m, 5H), 7.10 (d, $^1J_{HP}$ = 639 Hz, 1H), 2.70 (t, $^3J_{HH}$ = 7.6 Hz, 2H), 1.53 (m, 2H), 1.25 (m, 2H) 0.79 (t, $^3J_{HH}$ = 7.02 Hz, 3H). ^{31}P NMR (162 MHz, $CDCl_3$): δ 1.4 (d, $^1J_{PH}$ = 644 Hz). ESI-MS: $[C_{10}H_{18}NO_3P + H]^+$ 232.110 *m/z* (cal'd 232.1097 *m/z*), $[C_{10}H_{18}NO_3P + BuNH_3]^+$ 305.2004 *m/z* (cal'd *m/z* 305.1989 *m/z*), $[2(C_{10}H_{18}NO_3P) + H]^+$ 463.2145 *m/z* (cal'd 463.2121 *m/z*), $[2(C_{10}H_{18}NO_3P) + BuNH_3]^+$ 536.3038 *m/z* (cal'd 536.3013 *m/z*), $[2(C_{10}H_{18}NO_3P) + (O^-)(PhO)P(O)H + 2H^+]$ 621.2275 *m/z* (cal'd 624.2275 *m/z*), $[3(C_{10}H_{18}NO_3P) + H^+]$ 694.3158 *m/z* (cal'd 694.3073 *m/z*), $[3(C_{10}H_{18}NO_3P) + BuNH_3]^+$ 767.4016 *m/z* (cal'd 767.4037 *m/z*). T_{onset} = 125°C; T_{peak} = 181°C.

Synthesis of phenyl *H*-phosphonate phenylammonium salt, 4d.
1d (3.0 mmol, 0.57 mL) and aniline (3.0 mmol, 0.27 mL) were added to a round bottom flask equipped with a stir bar. The mixture was stirred at 80°C for 20 hours. After the reaction, solids precipitated and dichloromethane (DCM) was added to dissolve the solid. Hexane was added dropwise to form a layer on DCM. The mixture was allowed to recrystallize and the contents were filtered. The white-brownish crystals were collected, and dried under vacuum. Yield = 0.24 g (40%), mp = 116.4°C. Note this product degrades quite quickly in solution to an insoluble solid making characterisation a challenge (see **Figures S20-S22, S24**). ^{1}H NMR (400 MHz, $CDCl_3$): δ 7.00-7.38 (m, 10H), 7.04 (d, $^{1}J_{HP}$ = 668 Hz, 1H). ^{31}P NMR (162 MHz, $CDCl_3$): δ 2.1 (d, $^{1}J_{PH}$ = 664 Hz). T_{onset} = 113°C; T_{peak} = 161°C.

Kinetic monitoring of 1a-1d with benzyl amine.
H-phosphonate diester, **1** (**1a**: 0.02 mol, 1.80 mL; **1b**: 0.05 mol, 8.33 mL; **1c**: 0.03 mol, 3.90 mL; **1d**: 0.02 mol, 3.80 mL;) was added to a vial or 2 necked round bottom flask containing magnetic stir bar. **1** was brought to the appropriate temperature (20°C for **1a** and **1d** or 80°C for **1b** and **1c**). Benzylamine (**1a**: 0.02 mol, 2.20 mL; **1b**: 0.05 mol, 5.50 mL; **1c**: 0.03 mol, 4.20 mL; **1d**: 0.02 mol, 2.20 mL) was added and a stopwatch was started. 0.05 mL of the mixture was extracted using a pipette and transferred to an amber vial containing 0.45 mL $CHCl_3$. The amber vial was immediately stored in the fridge to stop the reaction. The samples were analyzed using ^{31}P NMR spectroscopy.
1a: The time points where 0.05 mL sample was extracted were: 4.0, 6.0, 15, 20, 30, 60, 80, 375, 1476 and 1735 min (see **Figures S25-S29**). ^{31}P NMR (162 MHz, $CDCl_3$): δ 11.5 (**2a**, dq, $^{1}J_{PH}$ = 619 Hz, $^{3}J_{PH}$ = 12 Hz), 14.2 (**5a**, ds, $^{1}J_{PH}$ = 696 Hz, $^{3}J_{PH}$ = 12 Hz).
1b: The time points where 0.05 mL sample was extracted were: 0.5, 2.0, 4.0, 6.0, 8.0, 10, 60, 300, 1440, 2880 and 7080 min (see **Figures S30-S32**). ^{31}P NMR (162 MHz, $CDCl_3$): δ 9.0 (**2b**, dt, $^{1}J_{PH}$ = 615 Hz, $^{3}J_{PH}$ = 8.2 Hz), 17.7 (**5b**, dp, $^{1}J_{PH}$ = 637 Hz, $^{3}J_{PH}$ = 9.6 Hz).
1c: The time points where 0.05 mL sample was extracted were: 10, 20, 60, 180, 300, 1440, 2760, 4200, 5640 and 10020 min (see **Figures S33-S39**). ^{31}P NMR (162 MHz, $CDCl_3$): δ 3.7 ((*i*-PrO)$_2$P(O)OH), 7.0 (**2c,** dd, $^{1}J_{PH}$ = 613 Hz, $^{1}J_{PH}$ = 9.5 Hz), 15.5 (**5c,** br d, $^{1}J_{PH}$ = 635 Hz), 26.9 (**6c**, dt).
1d: The reaction occurred much too fast to monitor over time as the starting material **1d** was already nearly used up when the first spectrum was taken after 4 min (see **Figures S40-S42**). ^{31}P NMR (162 MHz, $CDCl_3$): δ 6.6 (**2d,** d, $^{1}J_{PH}$ = 647 Hz), 9.2 (**5d,** dt, $^{1}J_{PH}$ = 716 Hz, $^{3}J_{PH}$ = 9.3 Hz), 15.7 (**9d,** d, $^{1}J_{PH}$ = 667 Hz), 17.7 (**8d,** ds, $^{1}J_{PH}$ = 647 Hz, $^{3}J_{PH}$ = 10.5 Hz), 128.0 ($P(OPh)_3$, s).

The effect of amine on the reaction.
For both **1b** and **1d**, two amines ($BnNH_2$ and *n*-$BuNH_2$) have been used to make the ionic salts **2b, 2d, 3b, 3d**. Two further reactions with the tertiary trimethylamine were completed for comparison.
10b: **1b** (5.0 mmol, 0.67 mL) and triethylamine (5.0 mmol, 0.70 mL) were added to a round bottom flask equipped with a stir bar. The mixture was stirred at 80°C for 20 hours. Conversion = 19% (see **Figures S43-S44**)
10d: **1d** (3.0 mmol, 0.57 mL) and triethylamine (3.0 mmol, 0.42 mL) were added to a round bottom flask equipped with a stir bar. The mixture was stirred at 80°C for 20 hours. Conversion = 14% (see **Figures S45-S46**).

Acknowledgements

K. L. L., J. F., T. S. and E. M. L. would like to acknowledge the School of Chemical Sciences and the MacDiarmid Institute for financial support. P.A.H. acknowledges support from the MacDiarmid Institute for a Personal Post-Doctoral Fellowship. All calculations were performed using the VUW High Performance Computing Cluster "Rāpoi". We thank Tatiana Groutso for collecting the single crystal X-ray diffraction data.

Keywords: *H*-phosphonate diesters • ionic salt • amine • mechanism • dealkylation

[1] a) K. Troev, *Chemistry and Application of H-Phosphonates*, Elsevier Science, **2006**, p vii-viii, 11-105,; b) M. K. Sobkowski, A.; Stawinski, J., *Top. Curr. Chem.* **2015**, *361*, 137-177.
[2] a) Y. B. Zhou, J. Yang, T. Q. Chen, S. F. Yin, D. Q. Han and L. B. Han, *Bull. Chem. Soc. Japan* **2014**, *87*, 400-402; b) M. Meazza, A. Kowalczuk, L. Shirley, J. W. Yang, H. Guo and R. Rios, *Adv. Syn. Cat.* **2016**, *358*, 719-723; c) J. Fraser, L. J. Wilson, R. K. Blundell and C. J. Hayes, *Chem. Commun.* **2013**, *49*, 8919-8921; d) X. J. Jin, K. Yamaguchi and N. Mizuno, *Org. Lett.* **2013**, *15*, 418-421; e) J. Q. Zhang, Y. S. Xiong, A. S. C. Chan and G. Lu, *RSC Adv.* **2016**, *6*, 84587-84591; f) G. Wang, Q. Y. Yu, S. Y. Chen and X. Q. Yu, *Tetrahedron Lett.* **2013**, *54*, 6230-6232; g) Y. J. Li and F. S. Liang, *Tetrahedron Lett.* **2016**, *57*, 2931-2934; h) G. Hong, X. Y. Zhu, C. Hu, A. N. Arum, S. Y. Wu and L. M. Wang, *J. Org. Chem.* **2016**, *81*, 6867-6874.
[3] Y. B. Zhou, S. F. Yin, Y. X. Gao, Y. F. Zhao, M. Goto and L. B. Han, *Angew. Chem. Int. Ed.* **2010**, *49*, 6852-6855.
[4] A. K. Purohit, D. Pardasani, A. Kumar, D. R. Goud, R. Jain and D. K. Dubey, *Tetrahedron Lett.* **2015**, *56*, 4593-4595.
[5] a) J. X. Wang, X. L. Wang, H. J. Li and J. Yan, *J. Organomet. Chem.* **2018**, *859*, 75-79; b) X. H. Zhang, D. G. Wang, D. An, B. S. Han, X. Song, L. Li, G. Q. Zhang and L. X. Wang, *J. Org. Chem.* **2018**, *83*, 1532-1537; c) H. Huang, J. Ash and J. Y. Kang, *Org. Biomol. Chem.* **2018**, *16*, 4236-4242.
[6] a) A. Kondoh and M. Terada, *Chem. Eur. J.* **2018**, *24*, 3998-4001; b) E. O. Yurko, T. V. Gryaznova, K. V. Kholin, V. V. Khrizanforova and Y. H. Budnikova, *Dalton Trans.* **2018**, *47*, 190-196; c) E. O. Yurko, T. V. Gryaznova, V. V. Khrizanforova, M. N. Khrizanforov, A. V. Toropchina, Y. H. Budnikova and O. G. Sinyashin, *Russ. Chem. Bull.* **2018**, *67*, 102-107; d) M. R. Patil, N. P. Dedhia, A. R. Kapdi and A. V. Kumar, *J. Org. Chem.* **2018**, *83*, 4477-4490; e) T. Q. Chen, C. Q. Zhao and L. B. Han, *J. Am. Chem. Soc.* **2018**, *140*, 3139-3155; f) W. B. Wu, Y. C. Wong, Z. K. Tan and J. Wu, *Catal. Sci.Technol.* **2018**, *8*, 4257-4263; g) B. Z. Lin, S. S. Shi, R. C. Lin, Y. Q. Cui, M. J. Fang, G. Tang and Y. F. Zhao, *J. Org. Chem.* **2018**, *83*, 6754-6761; h) L. Chen, X. Y. Fang and Y. X. Zou, *Org. Biomol. Chem.* **2018**, *16*, 951-956; i) W. C. Yang, K. Wei, X. Sun, J. Zhu and L. Wu, *Org. Lett.* **2018**, *20*, 3144-3147; j) A. Matsude, K. Hirano and M. Miura, *Org. Lett.* **2018**, *20*, 3553-3556; k) P. H. Li, G. W. Wang, X. J. Zhu and L. Wang, *Tetrahedron* **2019**, *75*, 3448-3455; l) C. Y. Li, T. Q. Chen and L. B. Han, *Dalton Trans.* **2016**, *45*, 14893-14897; m) H. Fu, T. Yang, J. Q. Shang, J. L. Zhou, M. Sun and Y. M. Li, *Org. Chem. Front.* **2017**, *4*, 1777-1780; n) Y. K. Yang, C. Qu, X. L. Chen, K. Sun, L. B. Qu, W. Z. Bi, H. Hu, R. Li, C. F. Jing, D. H. Wei, S. K. Wei, Y. Q. Sun, H. Liu and Y. F. Zhao, *Org. Lett.* **2017**, *19*, 5864-5867; o) J. Xu, P. B. Zhang, X. Q. Li, Y. Z. Gao, J. Wu, G. Tang and Y. F. Zhao, *Adv. Syn. Cat.* **2014**, *356*, 3331-3335.
[7] a) R. Karpowicz, J. Lewkowski, M. Stasiak, A. Czopor, P. Tokarz, A. Krol, D. Rogacz and P. Rychter, *Phosphorus Sulfur Silicon Relat. Elem.* **2018**, *193*, 423-436; b) D. T. Keough, D. Rejman, R. Pohl, E. Zbornikoa, D. Hockova, T. Croll, M. D. Edstein, G. W. Birrell, M. Chavchich, L. M. J. Naesens, G. K. Pierens, I. M. Brereton and L. W. Guddat, *ACS Chem. Bio.* **2018**, *13*, 82-90; c) A. Kraszewski and J. Stawinski, *Pure Appl. Chem.* **2007**, *79*, 2217-2227; d) M. Froneman and T. A. Modro, *Tetrahedron Lett.* **1988**, *29*, 3327-3330; e) A. B. Mirgorodskaya, L. Y. Zakharova, R. A. Shagidullina, L. A. Kudryavtseva, I. M. Shermergorn, V. E. Belskii and B. E. Ivanov, *Bull. Russ. Aca. Sci. Ussr Div. Chem. Sci.* **1990**, *39*, 1013-1017.
[8] a) K. Troev, S. Shenkov and U. Delimarinova, *Phosphorus Sulfur Silicon Relat. Elem.* **1992**, *68*, 107-114; b) S. Hossain, S. K. Gupta and R. Murugavel, *CrystEngComm* **2015**, *17*, 4355-4366; c) A. Lemeune, A. Y. Mitrofanov, Y. Rousselin, C. Stern, R. Guilard, Y. Y. Enakieva, Y. G. Gorbunova and S. E. Nefedov, *Phosphorus Sulfur Silicon Relat. Elem.* **2015**, *190*, 831-836; d) M. Blaha, M. Trchova, P. Bober, Z. Moravkova, Z. D. Zujovic, S. K. Filippov, J. Prokes, J. Pilar and J. Stejskal, *Syn. Met.* **2017**, *232*, 79-86; e) Z. Moravkova, M. Trchova, J. Dybal, M. Blaha and J. Stejskal, *J. Appl. Polym. Sci.* **2018**,

135; f) H. Busch, E. Schiebel, A. Sickinger and S. Mecking, *Macromolecules* **2017**, *50*, 7901-7910.
[9] a) B. G. Janesko, H. C. Fisher, M. J. Bridle and J. L. Montchamp, *J. Org. Chem.* **2015**, *80*, 10025-10032; b) W. J. Bailey and R. B. Fox, *J. Org. Chem.* **1963**, *28*, 531-534; c) J. Stawinski and A. Kraszewski, *Acc. Chem. Res.* **2002**, *35*, 952-960; d) E. E. Nifant'ev, *Russ. Chem. Rev.* **1978**, *47*, 835-858.
[10] a) B. Kurscheid, W. Wiebe, B. Neumann, H. G. Stammler and B. Hoge, *Eur. J. Inorg. Chem.* **2011**, 5523-5529; b) D. B. Vincze, P.; Abranyi-Balogh, P., *Phosphorus Sulfur Silicon Relat. Elem.* **2019**, *194*, 359-360; c) J. E. Griffiths and A. B. Burg, *J. Am. Chem. Soc.* **1960**, *82*, 1507-1508.
[11] a) K. A. G. t. Petrov, R. G., *Russ. Chem. Rev.* **1966**, *35*, 622-631; b) M. J. Gallagher and H. Honegger, *J. Chem. Soc. Chem. Commun.* **1978**, 54-55.
[12] a) F. H. Westheimer, *Acc. Chem. Res.* **1968**, *1*, 70-78; b) Z. Luz and B. Silver, *J. Am. Chem. Soc.* **1961**, *83*, 4518-4521; c) J. P. Guthrie, *J. Am. Chem. Soc.* **1977**, *99*, 3991-4001; d) M. C. Mitchell, R. J. Taylor and T. P. Kee, *Polyhedron* **1998**, *17*, 433-442; e) J. R. Peyser and J. P. Ferris, *Origins Life Evol. B.* **2001**, *31*, 363-380.
[13] A. Sobkowska, M. Sobkowski, J. Cieslak, A. Kraszewski, I. Kers and J. Stawinski, *J. Org. Chem.* **1997**, *62*, 4791-4794.
[14] K. L. Lee, J. Feld, Y. Ben-Tal, Z. Y. Guo, P. Hume and E. M. Leitao, *Asian J. Org. Chem.* **2019**, *8*, 1415-1425.
[15] a) V. Mitova, N. Koseva and K. Troev, *RSC Adv.* **2014**, *4*, 64733-64736; b) E. M. Georgiev, Kaneti, J., Troev, K., Roundhill, D. M., *J. Am. Chem. Soc.* **1993**, *115*, 10964-10973.
[16] a) D. E. Bryant, C. Kilner and T. P. Kee, *Inorg. Chim. Acta* **2009**, *362*, 614-616; b) M. D. M. Gray and D. J. H. Smith, *Tetrahedron Lett.* **1980**, *21*, 859-860; c) H. Krawczyk, *Synth. Commun.* **1997**, *27*, 3151-3161; d) N. S. Kumar, S. Kumaraswamy, M. A. Said and K. C. K. Swamy, *Org. Process Res. Dev.* **2003**, *7*, 925-928; e) K. Troev and R. Tsevi, *Phosphorus Sulfur Silicon Relat. Elem.* **1998**, *133*, 61-68; f) K. Troev, *Heteroat. Chem.* **2000**, *11*, 205-208.
[17] J. Pitawala, J. Scheers, P. Jacobsson and A. Matic, *J. Phys. Chem. B* **2013**, *117*, 8172-8179.
[18] a) A. E. Jimenez, A. Rossi, M. Fantauzzi, T. Espinosa, J. Arias-Pardilla, G. Martinez-Nicolas and M. D. Bermudez, *ACS Appl. Mater. Interfaces* **2015**, *7*, 10337-10347; c) T. Espinosa, J. Sanes and M. D. Bermudez, *Coatings* **2015**, *5*, 39-53; d) Y. Y. Han, D. Qiao, S. W. Zhang and D. P. Feng, *Tribol. Int.* **2017**, *114*, 469-477.
[19] a) J. Palgunadi, J. E. Kang, M. Cheong, H. Kim, H. Lee and H. S. Kim, *B. Korean Chem. Soc.* **2009**, *30*, 1749-1754; b) J. Palgunadi, J. E. Kang, D. Q. Nguyen, J. H. Kim, B. K. Min, S. D. Lee, H. Kim and H. S. Kim, *Thermochimica Acta* **2009**, *494*, 94-98.
[20] Y. Fukaya, R. Asai, S. Kadotani, T. Nokami and T. Itoh, *Bull. Chem. Soc. Jpn.* **2016**, *89*, 879-886.
[21] a) A. D. Dal-Maso, Legendre, F., Blonski, C., Hoffmann, P., *Synth. Commun.* **2008**, *38*, 1688-1693; b) B. Boutevin, Y. Hervaud, T. Jeanmaire, A. Boulahna and M. Elasri, *Phosphorus Sulfur Silicon Relat. Elem.* **2001**, *174*, 1-14; c) Y. Jin, M. Sun, H. Fu and Y. F. Zhao, *Chem. Lett.* **2004**, *33*, 116-117; d) A. Zwierzak and M. Kluba, *Tetrahedron* **1973**, *29*, 1089-1094.
[22] A. Kers, I. Kers, J. Stawinski, M. Sobkowski and A. Kraszewski, *Tetrahedron* **1996**, *52*, 9931-9944.
[23] a) K. Troev and D. M. Roundhill, *Phosphorus Sulfur Silicon Relat. Elem.* **1988**, *37*, 243-245; b) E. M. Georgiev, R. Tsevi, V. Vassileva, K. Troev and D. M. Roundhill, *Phosphorus Sulfur Silicon Relat. Elem.* **1994**, *88*, 139-145; c) V. Vassileva, E. M. Georgiev, K. Troev and D. M. Roundhill, *Phosphorus Sulfur Silicon Relat. Elem.* **1994**, *92*, 101-107.
[24] S. Hossain, Gupta, S. K., Murugavel, R., *CrystEngComm* **2015**, *17*, 4355-4366.
[25] M. L. Williams, S. P. Holahan, M. E. McCorkill, J. S. Dickmann and E. Kiran, *Thermochim. Acta* **2018**, *669*, 126-139.
[26] Y. Y. Cao and T. C. Mu, *Ind. Eng. Chem. Res.* **2014**, *53*, 8651-8664.
[27] a) A. D. Becke, *Phys. Rev. A* **1988**, *38*, 3098-3100; b) A. D. Becke, *J. Chem. Phys.* **1993**, *98*, 5648-5652; c) C. Lee, Yang, W., Parr, R. G., *Phys. Rev. B.* **1988**, *37*, 785-789.
[28] S. Grimme, J. Antony, S. Ehrlich and H. Krieg, *J. Chem. Phys.* **2010**, *132*.
[29] C. Coquery, F. Carosio, C. Negrell, N. Causse, N. Pebere and G. David, *Surf. Interfaces* **2019**, *16*, 59-66.
[30] G. M. Sheldrick, *Acta Crystallogr. C* **2015**, *71*, 3-8.
[31] O. V. Dolomanov, L. J. Bourhis, R. J. Gildea, J. A. K. Howard and H. Puschmann, *J. Appl. Crystallogr.* **2009**, *42*, 339-341.
[32] C. F. Macrae, P. R. Edgington, P. McCabe, E. Pidcock, G. P. Shields, R. Taylor, M. Towler and J. van De Streek, *J. Appl. Crystallogr.* **2006**, *39*, 453-457.
[33] M. J. Frisch; G. W. Trucks; H. B. Schlegel; G. E. Scuseria; M. A. Robb; J. R. Cheeseman; G. Scalmani; V. Barone; B. Mennucci; G. A. Petersson; H. Nakatsuji; M. Caricato; X. Li; H. P. Hratchian; A. F. Izmaylov; J. Bloino; G. Zheng; J. L. Sonnenberg; M. Hada; M. Ehara; K. Toyota; R. Fukuda; J. Hasegawa; M. Ishida; T. Nakajima; Y. Honda; O. Kitao; H. Nakai; T. Vreven; J. A. Montgomery Jr. ; J. E. Peralta; F. Ogliaro; M. Bearpark; J. J. Heyd; E. Brothers; K. N. Kudin; V. N. Staroverov; R. Kobayashi; J. Normand; K. Raghavachari; A. Rendell; J. C. Burant; S. S. Iyengar; J. Tomasi; M. Cossi; N. Rega; J. M. Millam; M. Klene; J. E. Knox; J. B. Cross; V. Bakken; C. Adamo; J. Jaramillo; R. Gomperts; E. Stratmann; O. Yazyev; A. J. Austin; R. Cammi; C. Pomelli; J. W. Ochterski; R. L. Martin; K. Morokuma; V. G. Zakrzewskil; G. A. Voth; P. Salvador; J. J. Dannenberg; S. Dapprich; A.D. Daniels; Ö. Farkas; J. B. Foresman; J. V. Ortiz; J. Cioslowski; D. J. Fox; Gaussian, Inc.: Wallingford CT, 2013.

10.1002/chem.202003090

WILEY-VCH

FULL PAPER

Entry for the Table of Contents

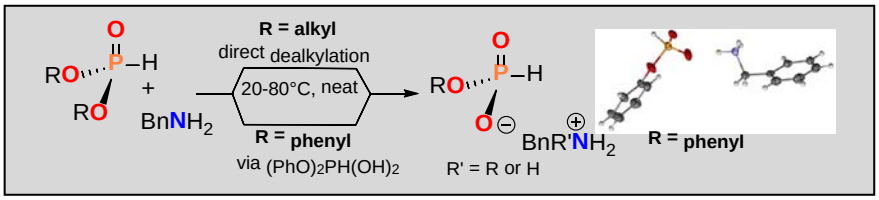

I on it. Dialkyl and diphenyl *H*-phosphonates undergo dealkylation and dearylation, respectively, upon heating with amines to afford the corresponding ionic salts. The mechanisms for these processes, which form ammonium monosubstituted *H*-phosphonate salts held together by H-bonds, were interrogated both experimentally and theoretically, and the results show that they are very different.

Institute and/or researcher Twitter usernames: @MacDiarmidInsti